Available online at www.sciencedirect.com

ScienceDirect

Energy Procedia 124 (2017) 295–301

Energy Procedia

www.elsevier.com/locate/procedia

7th International Conference on Silicon Photovoltaics, SiliconPV 2017

Effect of the SiO_2 interlayer properties with solid-source hydrogenation on passivated contact performance and surface passivation

Bill Nemeth[a], Steven P. Harvey[a], Jian V. Li[b], David L. Young[a], Ajay Upadhyaya[c], Vincenzo LaSalvia[a], Benjamin G. Lee[a], Matthew R. Page[a], Paul Stradins[a]

a NREL, 15013 Denver West Parkway, Golden, CO, 80401, USA
b Texas State University, 601 University Drive, San Marcos, TX, 78666, USA
c Georgia Institute of Technology, North Ave NW, Atlanta, GA 30332

Abstract

We investigate how SiO_x oxide interlayers prepared by different techniques (chemical, thermal) in combination with hydrogen released from an ALD Al_2O_3 source layer govern passivation in 1) passivated contacts based on doped poly-Si layers and tunneling SiO_2, and 2) wafer surface passivation by Al_2O_3. Profiles of O and H in these structures with engineered, buried SiO_x interlayers were measured by Time-of-Flight SIMS (TOF-SIMS) at nanometer resolution. Passivated contacts perform best with thermally oxidized SiO_x, while chemical SiO_x causes poly-Si film blistering and performance degradation. ALD Al_2O_3 acts as passivating H source, significantly improving B-doped and intrinsic poly-Si contacts for IBC cells. Fast-diffusing hydrogen from the Al_2O_3 source layer appears to penetrate Si wafer thickness, improving the passivation of structures at the opposite side. In contrast to the passivated contacts, chemical SiO_x interlayer promotes wafer surface passivation by ALD Al_2O_3, while similarly thin thermal SiO_2 suppresses passivation and built-in charge.

Peer review by the scientific conference committee of SiliconPV 2017 under responsibility of PSE AG.

Keywords: silicon; passivation; passivated contact; polysilicon; Al_2O_3

1. Introduction

In passivation of Si interfaces, contacts, and bulk for efficient solar cells, oxygen and hydrogen play significant roles. Here, we examine passivation by interfacial SiO_2 and by hydrogen in: 1) passivated contacts with heavily doped poly-Si layers separated from the wafer by thin SiO_2; and 2) wafer surface passivation by Al_2O_3. A thin

1876-6102
Peer review by the scientific conference committee of SiliconPV 2017 under responsibility of PSE AG.
10.1016/j.egypro.2017.09.302

tunneling SiO_2 interlayer enables the above passivating contact. Conversely, passivation of wafer surfaces by Al_2O_3 is governed by interfacial SiO_x formed spontaneously at 400°C [1] or inserted as a SiO_x interlayer [2]. Both passivated contact [3] and surface passivation [1] further improves by hydrogen released from the ALD Al_2O_3. Maximizing performance of n-, i-, and p-type passivated contacts by engineering the tunneling SiO_x layer and solid-source hydrogenation is important for efficient IBC cells. Comparing the same interfacial SiO_x in both surface and contact passivation helps elucidate passivation mechanisms.

2. Experimental

Thin oxide layers for surface passivation with Al_2O_3 were grown on 2 Ω-cm p-FZ polished wafers chemically (room temperature HNO_3 (NAOS); Piranha; RCA) and thermally ("low temperature" oxide [3] in tube furnace at 700°C to ~1.4 nm, or at 1100°C and thinned to 4 nm in HF). Oxidized twin samples were UV-O_3 treated prior to ALD. Symmetric passivated contact structures on 200 micron thick n-Cz (4 Ω–cm) wafers had 1.4 nm "low temperature" SiO_2 and ~50 nm a-Si:H by PECVD, then thermally crystallized to poly-Si in N_2 at 850°C. Finally, both p-FZ oxidized wafers and n-Cz contacts received ALD Al_2O_3 and were annealed 20 min at 400°C [3]. Implied open circuit voltage (iV_{oc}) was measured by Sinton WCT-120 and the built-in charge extracted from C-V. Nanometer resolved TOF-SIMS used 30 keV Bi primary and 1 keV Cs sputtering ions.

3. Results and discussion

3.1. p-FZ Si wafer surface SiO_x treatments and effect of passivation with ALD Al_2O_3

Wafer surface passivation of Al_2O_3 with various SiO_x stacks are shown in Figure 1 and Table 1 (inset). Here, samples with the SiO_x interlayer formed chemically, "natively", or even with the oxide absent result in high iV_{oc} and more negative fixed charge than with the SiO_x interlayer grown thermally at 700°C ("thermal") or at 1100°C ("thinned"). Note that the thickest chemical oxides (NAOS and its UV/ozonated version) have approximately the same thickness ~1.3 nm as the 700°C thermal oxide, yet they yield higher iV_{oc} and fixed negative charge values.

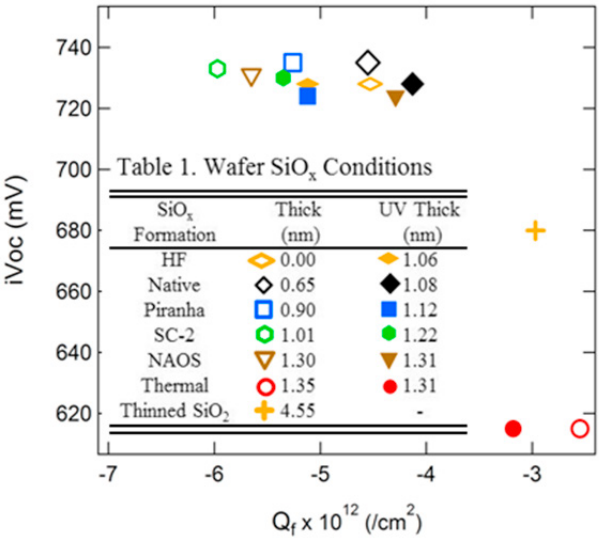

Fig. 1. iV_{oc} vs. fixed charge (Q_f) of Al_2O_3 on various SiO_x of Table 1, without (open symbols) and with (solid symbols) UV-O_3 exposure.

TOF-SIMS resolves the SiO_x layer within the $Al_2O_3/SiO_x/Si$ stack by detecting sputtered species of O bonded to Si (Figure 2), as well as H bonded to Si. The "chemical" SiO_x contains less O (compare SiO_2^+ species

peaks) and more H (SiH^+ species) than its thermal 700°C SiO_x counterpart. The SiH^+ signal is shifted towards the wafer in both cases and coincides with the sub-stoichiometric Si_2O^+ (red) peak, possibly indicating a defective, passivated interface. The relation of sputtered Si_xO_y species to the buried oxide stoichiometry in TOF-SIMS can be linked to interfacial versus bulk behavior [4]. These results have practical processing implications for the ALD Al_2O_3 passivation. Qualitatively, we observed robust passivation with chemical oxide interlayer as opposed to HF-dipped wafers, in cases when the ALD reactor was contaminated with sulfur-containing precursors.

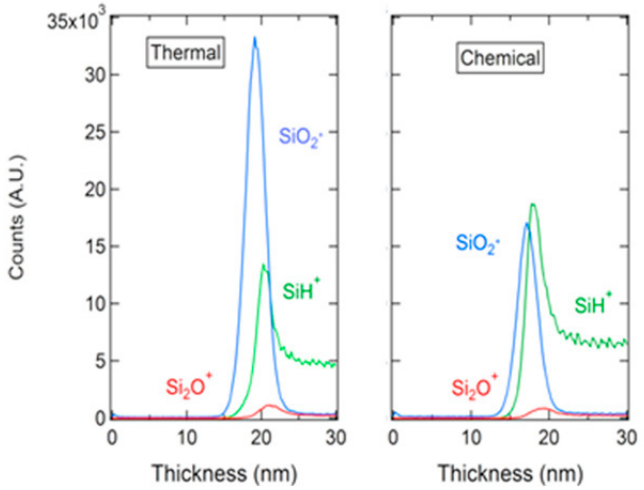

Fig. 2. TOF-SIMS of SiO_2^+, Si_2O^+, and SiH^+ species for Al_2O_3 annealed at 400°C in N_2 with thermal SiO_x (left) and chemical SiO_x (right).

3.2. Polysilicon passivated contacts and their passivation with ALD Al_2O_3 hydrogen source layer

Passivated contacts with various SiO_x and hydrogenation from the ALD Al_2O_3 exhibit robust performance and the highest iV_{oc} with thermally grown SiO_x tunneling layer. In contrast, PECVD of a-Si:H on the OH-rich chemical SiO_x often results in blistering, likely due to weak adhesion with enhanced hydrogen insertion at the SiO_x interface. Crystallization at 850°C promotes further blistering [5] due to hydrogen effusion. After metallization, these blistered films show 60-80 mV drop in iV_{oc}. In non-blistered films, annealing to ~850°C (well above crystallization at ~ 670 °C) improves contact performance. TOF-SIMS in Figure 3 shows depth profiles of various sputtered compound species involving silicon, oxygen, and hydrogen. The tunneling oxide region is represented by peaks in SiO_2^+, SiO_3^+, and Si_2O^+. Comparing the O-related profiles in the same passivated contact structure before and after the a-Si:H crystallization anneal at 850°C, we note appreciable "sharpening" of SiO_x layer edges after the 850°C anneal. The changes and sharpening are especially pronounced in the SiO_3^+ profile. Since the a-Si:H / poly-Si in Figure 3 is intrinsic (i.e. the dopants are not involved in the oxide modification), and SiO_x was grown thermally at 700°C, we conclude that the observed reconstruction and densification of the SiO_x and its interface with wafer enhances contact performance after 850°C treatment.

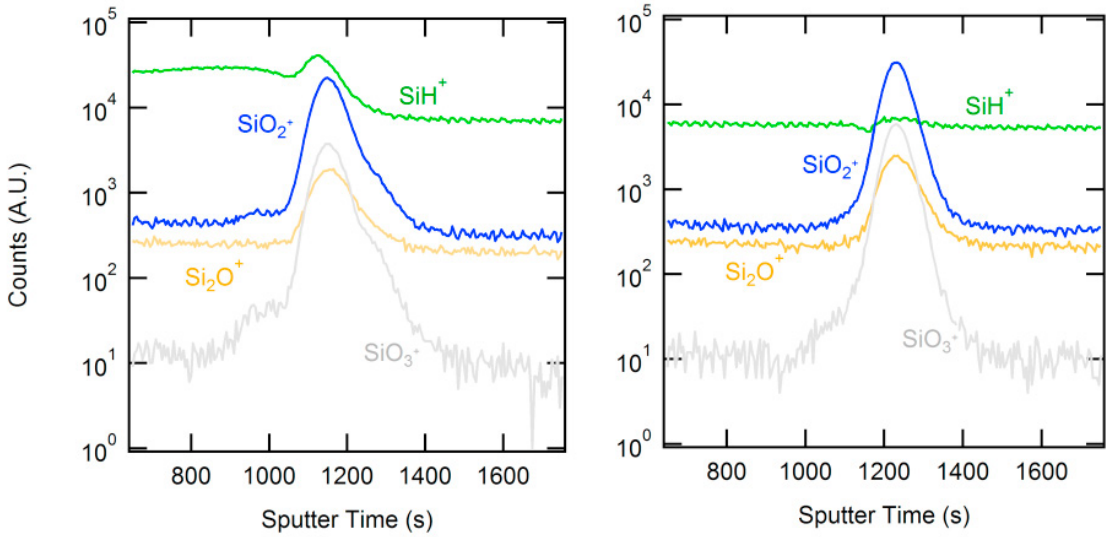

Fig. 3. TOF-SIMS profiles of SiH^+, SiO_2^+, SiO_3^+, Si_2O^+ sputtered species ratio for passivated contact structure before (left) and after (right) thermal crystallization at 850°C.

Passivated contacts are further improved by hydrogen released from ALD Al_2O_3 by annealing to 400°C in N_2 and penetrating into the poly-Si and reaching the tunneling oxide interfaces [3]. Here, this solid-source hydrogenation was realized in two different ways shown in Figure 4: "direct" and "indirect". The direct way involves ALD-depositing Al_2O_3 on the n+ poly layer of the passivated contact, thus releasing the H directly into the poly-Si and passivation the tunneling oxide interfaces as well. The indirect passivation involves depositing Al_2O_3 only on one side of the wafer, leaving its other side with the poly-Si passivated contact on it, without Al_2O_3. Furthermore, two sample structures were used to test these two ways of passivation: 1) a symmetric structure with passivated contacts on both sides and 2) passivated contact on one side, and Al_2O_3 directly on wafer on the other side. The resulting values of the iV_{oc} for these structures after the passivation (which includes the Al_2O_3 deposition and annealing at 400°C in N_2) are shown in the Figure 4. Before the ALD deposition, the measured iV_{oc} value for a symmetric poly-Si structure is approximately 680mV. After passivation using the "direct" way (Figure 4 a, b), high values of 738 and 736 mV are achieved. Somewhat surprisingly, the "indirect" passivation results in iV_{oc} values only 10 mV below those obtained "directly". This small difference in the iV_{oc} cannot be explained by just passivating a single side of the structure. Indeed, the total diode current prefactor J_o of the single-side passivated structure (c and d) is estimated to be larger than that of the double-side structure (a and b) by a factor of exp(10mV / kT) = 1.5. Since the "direct" passivated structure (a) exhibits total J_o of ~ 6 fA/cm^2, the "indirect" structure (c) should be passivated with total J_o of about 10 fA/cm^2, therefore, the wafer side without the Al_2O_3 is expected to have J_o <10 fA/cm^2. This low J_o value is not consistent with the measured iV_{oc} ~ 690 mV and $2J_o$ ~ 30fA/cm^2 values for the unpassivated poly-Si contact structure. We therefore suggest that the high iV_{oc} value of 728 mV in Figure 4d is a result of possible hydrogen migration through the wafer thickness, improving the passivation of the poly-Si/SiO_2 layer structures on the opposite side of the wafer.

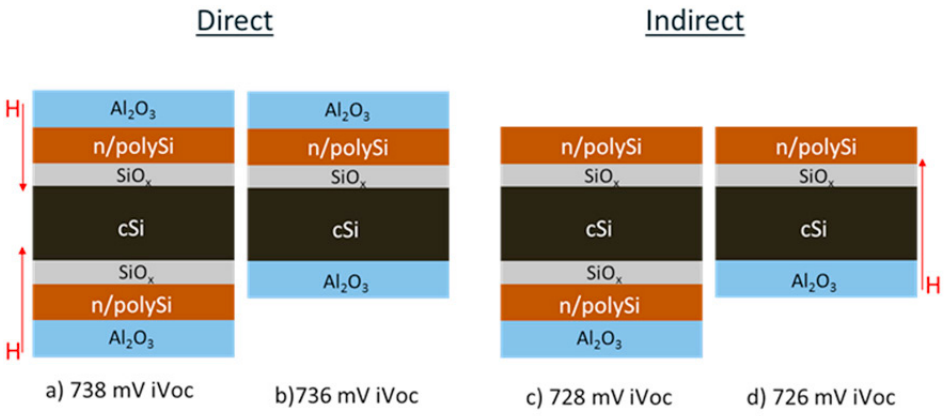

Fig. 4. Test structures for direct and indirect hydrogenation of passivated contact annealed in N_2, with final iV_{oc} values shown below each structure.

To further investigate this possibility, we performed SIMS study of the structures (a) and (d) of Figure 4. The corresponding H^+ profiles along with the SiO_2^+, taken from the poly-Si side, are shown in Figure 5. Structure (a) shows a significant overall H^+ signal and a H^+-peak near the tunneling oxide. In the structure (d), the H^+-signal is still visible near the poly-Si, with a similar but lower H^+-peak near the tunneling oxide. This suggests that some H diffuses though the wafer to passivate the contacts on the other side. The amount of diffused H is likely small, but could possibly be increased by thinning the wafer and increasing the annealing temperature above 400ºC.

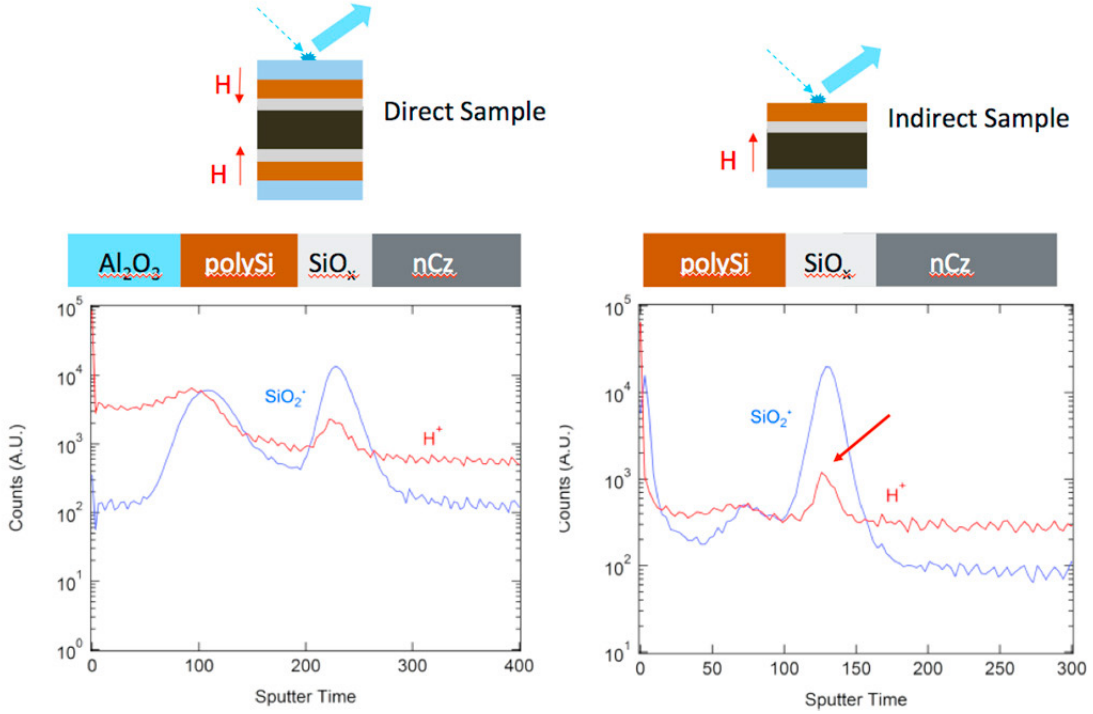

Fig. 5. TOF-SIMS profiles of SiH^+ and SiO_2^+ sputtered species direct and indirect hydrogenation of passivated contact.

The possibility of H diffusion through the wafer is reasonably consistent with the literature. Many groups have used numerous techniques to measure H-diffusion in silicon, with resulting diffusion coefficient values varying over 5 orders of magnitude, depending on doping, H-clustering and H_2 formation, measurement technique, etc.[7]. The upper limit of the measured H-diffusion coefficients are represented by the Schottky barrier capacitance results of Seager, et al. [6] and H-permeation data of Van Wieringen and Warmoltz [8]. The latter were obtained above 1000 ºC, where the Fermi-level position is near midgap in c-Si. This is similar to our experiment, where the n-Cz wafer doped to ~ $2x10^{15}$ cm^3 also becomes intrinsic around 300 ºC [9]. Extrapolated from [6] and [8], the H-diffusion coefficient at 400 ºC is around $2x10^{-6}$ cm^2/s. The diffusion length of H into our Si wafer can be estimated as:

$$x = \sqrt{D_H t}$$

In our experiment, the annealing time at 400 ºC is 20 minutes and the Eq. (1) with the above D_H value gives the diffusion length x of about 500 µm, which exceeds our wafer thickness of 180 µm. This appears consistent with our observation of partial involvement of H-diffusing through the wafer, to contribute to passivation of the poly-Si/SiO_2 structure.

Finally, we performed a control experiment to establish that no extra passivation is provided to the contact by depositing Al_2O_3 layer and then removing it by HF, as on the top side of the wafer in Figure 4c. For this, we prepared a symmetric n+ poly-Si/SiO_2 structure on n-Cz wafer including annealing it at 850 ºC. Then we processed it in three different ways and measured its iV_{oc}: 1) no Al_2O_3 deposition, no anneal at 400 ºC; 2) no Al_2O_3 deposition, with anneal at 400 ºC; 3) Al_2O_3 deposition, strip it off with HF, then anneal at 400 ºC; and 4) Al_2O_3 deposition, followed by anneal at 400 ºC. We also performed sequences (3) and (4) with p+ poly-Si passivated contacts on n-Cz wafer. The results are shown in Figure 6.

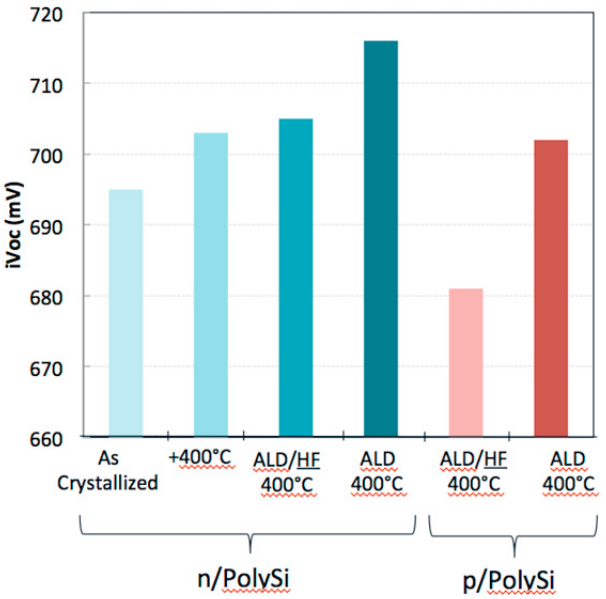

Fig 6. iV_{oc} values on n-type and p-type tunneling passivated contacts to n-Cz wafer after different processing sequences following crystallization anneal (details see text).

Figure 6 results suggest that ALD deposition and then removing the Al_2O_3 layer does not provide additional H for passivating the contacts. We do see some improvement after annealing at 400 ºC after sequence (3), but it is about the same as after sequence (2) without any Al_2O_3. Possibly, 20 min annealing at 400 ºC has some beneficial effect to the contact interface. In p-type contact, we see robust 20 mV difference between sequences (3) and (4), again confirming no residual passivation effect after removing Al_2O_3 layer prior to 400 ºC anneal.

We have used hydrogenation from the sacrificial Al_2O_3 layer to other combinations of wafer and poly-Si contact doping types, besides n-type poly-Si passivated contact to n-Cz wafer,. In all cases studied (see Table 2) the solid-state H-passivation significantly improves passivated contact properties to n-Cz wafer, especially in B-doped p-type and n-type poly-Si contacts, deposited either by PECVD or by LPCVD. In addition, we have achieved high iV_{oc} values for intrinsic poly-Si/SiO_2 layers. This is important for highly efficient IBC cells, where well-passivated n-, p-fingers can be separated by insulating, passivating intrinsic poly-Si gap layer. Finally, high iV_{oc} values of p-poly Si passivated contacts on p-Cz wafer would enable efficient BSF alternative for the p-PERC cells.

Table 2. Effect of solid-source hydrogenation on passivated contacts.

Condition	n-type on nCz by PECVD,iV_{oc} (mV)	p-type on nCz by PECVD, iV_{oc} (mV)	Intrinsic on nCz by PECVD, iV_{oc} (mV)	Intrinsic on nCz by LPCVD, iV_{oc} (mV)	p-type on pFZ by PECVD, iV_{oc} (mV)
After 850°C anneal	679	656	550	538	679
ALD Al_2O_3 + anneal	735	714	717	720	700

4. Conclusions

SiO_2 interlayer properties differently affect wafer surface passivation by Al_2O_3 and passivated contacts. Chemical SiO_2 enables excellent wafer surface passivation, while thermal SiO_2 enables robust passivated contact. H thermally released from ALD Al_2O_3 principally improves n-, p-type, and intrinsic poly-Si contacts on n-Cz wafer and p-type BSF contact on a p-Cz wafer. Some passivating hydrogen released from the Al_2O_3 appears to penetrate the wafer thickness at 400°C, improving passivated contacts on the opposite side of the wafer.

Acknowledgements

This work was supported by the U.S. Department of Energy under Contract DE-AC36-08-GO28308 to NREL.

References

[1] G. Dingemans and W. M. M. Kessels, “Status and prospects of Al_2O_3-based surface passivation schemes for silicon solar cells”, Journal of Vacuum Science & Technology A 30(4) 040802, (2012).
[2] V. Naumann, M. Otto, R. B. Wehrspohn, M. Werner, and C. Hagendorf, “Interface and material characterization of thin ALD-Al_2O_3 layers on crystalline silicon”, Energy Procedia 27 312, (2012).
[3] B. Nemeth, B., D. L. Young, M. R. Page, V. LaSalvia, S. Johnston, R. Reedy, and P. Stradins, “Polycrystalline silicon passivated tunneling contacts for high efficiency silicon solar cells”, Journal of Materials Research 31(06) 671 (2016).
[4] K. Chiba and S. Nakamura, “Characterization of ion species of silicon oxide films using positive and negative secondary ion mass spectra”, Applied Surface Science 253(2) 412, (2006).
[5] J.A. Aguiar, D.L. Young, B.G. Lee, W. Nemeth, S. Harvey, T. Aoki, M. Al-Jassim, and P. Stradins, “Atomic scale understanding of poly-Si/SiO_2/c-Si passivated contacts: passivation degradation due to metallization”, 43rd IEEE PVSC, Portland, OR, USA, 2016, MePVSC223_0608064721 (2016).
[6] C. H. Seager, R. A. Anderson, and D. K. Brice, “In situ measurements of hydrogen motion and bonding in silicon”, Journal of Applied Physics 68 3268 (1990).
[7] M. Stavola, “Hydrogen diffusion and solubility in c-Si,” in *Properties of Crystalline Silicon*, no. 9, R. Hull, Ed. London. 1999, p. 1016.
[8] A. Van Wieringen and N. Warmoltz, “On the permeation of hydrogen and helium in single crystal silicon and germanium at elevated temperatures,” *Physica*, 22(6), 849 (1956).
[9] S.M. Sze and K.K. Ng, (n.d.). Physics of semiconductor devices. 2007, Hoboken. New Jersey: John Wiley & Sons.